

An improved PageRank algorithm for art appreciation model design

Jingyao Chen ^{Corresp. 1}

¹ The Graduate School of Namseoul University, Cheonan, Republic of Korea

Corresponding Author: Jingyao Chen
Email address: chenjingyao1102@163.com

Aiming at the problem of extracting emotional characteristics in art appreciation, this paper puts forward an innovative method. Firstly, the PageRank algorithm is enhanced using tweet content similarity and time factors; Secondly, the SE-ResNet network design is used to integrate Efficient Channel Attention (ECA) with the residual network structure, and ResNeXt50 is optimized to enhance the extraction of image sentiment features. Finally, the weight coefficients of overall emotions are dynamically adjusted to select a specific emotion incorporation strategy, resulting in effective bimodal fusion. The proposed model demonstrates exceptional performance in predicting sentiment labels, with maximum classification accuracy reaching 88.20%. The accuracy improvement of 21.34% in comparison to traditional Deep Convolutional Neural Networks (DCNN) model attests to the effectiveness of this study. This research enriches the emotion feature extraction capabilities of image and text and improves the accuracy of emotion fusion classification.

1 An improved PageRank algorithm for art appreciation 2 model design

3
4 Jingyao Chen*

5
6 The Graduate School of Namseoul University; Cheonan 31020; Republic of Korea;

7
8 *Corresponding Author:

9 Jingyao Chen;

10 No. 91, Daehangro, Seonghwan-eup, Cheonan

11 Email address: chenjingyao1102@163.com

12

13 Abstract

14 Aiming at the problem of extracting emotional characteristics in art appreciation, this paper puts
15 forward an innovative method. Firstly, the PageRank algorithm is enhanced using tweet content
16 similarity and time factors; Secondly, the SE-ResNet network design is used to integrate Efficient
17 Channel Attention (ECA) with the residual network structure, and ResNeXt50 is optimized to
18 enhance the extraction of image sentiment features. Finally, the weight coefficients of overall
19 emotions are dynamically adjusted to select a specific emotion incorporation strategy, resulting in
20 effective bimodal fusion. The proposed model demonstrates exceptional performance in
21 predicting sentiment labels, with maximum classification accuracy reaching 88.20%. The
22 accuracy improvement of 21.34% in comparison to traditional Deep Convolutional Neural
23 Networks (DCNN) model attests to the effectiveness of this study. This research enriches the
24 emotion feature extraction capabilities of image and text and improves the accuracy of emotion
25 fusion classification.

26 **Keywords:** PageRank; ResNeXt50; ECA; art appreciation; sentiment classification

27

28 1. Introduction

29 Artists use effective integration of their creative techniques and shapes in their artwork to
30 convey the content of their art. This approach not only effectively expresses the emotions of the
31 artwork, but also exceeds the limitations of traditional art language in conveying emotions.
32 Emotions in interactive art encompass not only the emotions of the creator, but also the emotions
33 of the participants involved in the interaction ^[1-2]. Therefore, artists must not only convey their
34 emotions through artistic techniques, but also possess a thorough understanding of the
35 psychological emotions of the participants. This enables them to effectively convey their emotions

36 to the participants and create an immersive artistic experience.
37 With the rapid increase in visual information, there is a growing demand for image sentiment
38 processing and analysis. Sentiment analysis plays a crucial role in understanding human
39 emotional experiences with images^[3]. In interactive art appreciation, a significant "emotional gap"
40 exists between images and emotions due to the challenge of connecting pixel-level visual
41 information to the complex and high-level mental process of emotions^[4]. The ambiguity of
42 interactive art originates from its emotional nature, which has been an area of interest for artificial
43 intelligence research, including image aesthetic quality evaluation^[5], stylized image description
44 generation^[6] and visual semantic segmentation^[7]. Since both emotion and aesthetics are
45 subjective and abstract, methods from both fields can be utilized interchangeably in image
46 aesthetic quality evaluation. In stylized image description generation, sentiment prediction for
47 images can assist in generating image descriptions with sentiment tendencies. Furthermore, in
48 multimedia content filtering and recommendation, users can select specific sentiments for
49 corresponding image search based on their past sentiment preferences, resulting in an improved
50 aesthetic experience for visual participants.
51 Early scholars, drawing inspiration from the fields of psychology and aesthetics, crafted
52 conventional manual features in order to predict the emotions that images evoke^[8-9]. Some
53 experts have contended that emotions may be highly interrelated with certain isolated features
54 and have endeavored to establish associations between them, relying on human cognition or
55 associated theories. These investigations typically involve the extraction of image features, such
56 as color, texture, composition, and content, which are then integrated to forecast sentiment^[10].
57 One may depict image emotions by combining generic features and artistic element features at
58 the low level, attribute features and artistic principle features at the middle level, and semantic
59 features and face features at the high level. At present, the primary avenue for art learners to
60 obtain images is through web pages, which yield an enormous amount of visual data and
61 information due to the large number of online community users and fast-paced knowledge
62 dissemination. By analyzing link relationships between web pages and combining them with user
63 search topics, they can offer users more comprehensive and precise information^[11]. Furthermore,
64 recognition of different user activity and interaction emotional tendencies can determine the rating
65 and appreciation effects of art images. A novel and efficient representation learning technique for
66 a myriad of image appreciation tasks through convolutional neural networks (CNNs) has been
67 extensively researched^[12-14]. This method introduces the PageRank model to examine the
68 original sentiment tendency of the participants' comment vocabulary, aiding in the accurate
69 identification and promotion of their art appreciation behavior.

70

71 **2. Related works**

72 **2.1 PageRank Algorithm**

73 The PageRank algorithm has become a prevalent ranking algorithm that is widely employed
74 in search scenarios where diverse datasets can be represented as graph structures, such as Web
75 search^[15], ER graph search^[16], and keyword database search^[17]. The personalized PageRank

76 algorithm inherits the principles of the classical PageRank algorithm and employs the data model
77 (graph) link structure to recursively calculate the weight of each node. This algorithm simulates
78 the user's behavior of randomly visiting nodes in the graph by clicking on links, i.e., it follows a
79 random walk model to calculate the probability of random visits to each node in the steady state.
80 The personalized PageRank algorithm accounts for not only the static link structure between
81 nodes when calculating node weights, but also the user preferences expressed in personalized
82 information, such as user queries, favorite pages, and so on^[18].

83 The accuracy of existing PageRank algorithms is determined by the configuration of static
84 parameters, such as the number of Fingerprints and the selection of hub nodes, which cannot be
85 dynamically adjusted at runtime^[19]. Additionally, the algorithm's running efficiency is directly
86 determined by the precision requirements set during compilation and cannot be dynamically
87 tuned. Nevertheless, since different users or applications have varying efficiency and accuracy
88 demands for algorithms, estimation algorithms that support run-time tuning of efficiency and
89 accuracy, such as incremental optimization, are imperative^[20]. Some scholars have proposed an
90 improvement method based on user interest that involves collecting and analyzing user usage
91 data to determine the direction of user interest, which can enhance the accuracy of recommended
92 content^[15]. Another improvement approach is to start from page similarity, which is currently
93 classified into two main categories^[21-22]: one uses the space vector model to determine the
94 similarity between the page and the linked page, assigning more weight to the page with greater
95 similarity to solve the problem of average weights; the other is an improved method based on
96 content filtering, which evaluates page text and HTML tags to make the query results more
97 precise.

98

99 2.2 Visual sentiment analysis

100 Image sentiment analysis can be categorized into two approaches: visual features and
101 semantic features. Zhu et al.^[23] defined 102 mid-level semantic representations for image
102 sentiment analysis, which resulted in better sentiment prediction results than using visual low-
103 level features alone. Zhao et al.^[24] proposed a sentiment analysis approach based on designing
104 visual art sentiment subjects and corresponding visual art sentiment patterns based on different
105 types of sentiment subjects. Other research has focused on learning the affective distribution of
106 visual art affective patterns and further describing visual art characteristics. One feasible method
107 is to calculate the overall sentiment value of an image based on textual sentiment values of
108 adjective-noun pairs and corresponding responses in the image. Jiang et al.^[25] constructed a
109 strongly and weakly supervised coupled network system for visual sentiment differentiation of
110 images by importing images into VGGNet and obtaining the entire image features from the fifth
111 convolutional layer, and then using a spatial pooling strategy to obtain weights for each emotion
112 type. Li et al.^[26] proposed a 3D CNN combining 3D Inception-ResNet layer and LSTM network to
113 extract spatial features of the image using Inception ResNet and learn temporal relationships
114 using LSTM, and then apply this information for classification.

115

116 3. Methodology

117 Figure 1 depicts the overarching framework of the sentiment analysis model for art
118 appreciation that is utilized in this study. The framework comprises of four distinct components:

119 (1) Data Importation: The dataset is procured from various microblogs, Twitter, and other
120 media platforms. The crawler tools acquire a substantial amount of text and image data, which is
121 preprocessed into input samples. All the samples are defined as $S(T_i, I_i)$, where T_i and I_i represent
122 all text and images of the i th sample, respectively.

123 (2) Feature Extraction: The improved PageRank algorithm and ECA+ResNeXt50 is used for
124 text and image sentiment feature extraction, respectively. Text features $T_i=(T_1, T_2, \dots, T_m)$ and
125 image features $I_i=(I_1, I_2, \dots, I_n)$ are obtained separately using each component, where m and n
126 denote the dimensions of textual and graphical features, respectively.

127 (3) Feature Fusion: Firstly, an appropriate fusion strategy is determined based on the
128 statistical sentiment contribution of each modality towards the overall sentiment. Then, cross-
129 modal learning algorithms are employed to fuse the features and compute the statistical sentiment
130 weights between the characteristics of the two modalities.

131 (4) Sentiment Analysis: Lastly, the trained cross-modal learning algorithm is utilized to
132 achieve sentiment classification of graphical texts.

133

134 Figure 1. Art appreciation sentiment analysis model

135

136 3.1 Text Emotion Feature Extraction Based on PageRank Algorithm

137 3.1.1 Algorithm description

138 Let the seed sentiment word set vector be $S = \{s_1, s_2, \dots, s_n\}$, whose manually labeled sentiment
139 polarity vector is $Y_S = \{y_1, y_2, \dots, y_n\}$; the vector of sentiment words to be classified is $W =$
140 $\{w_{n+1}, w_{n+2}, \dots, w_{n+m}\}$, the annotation result to be found is $Y_W = \{y_{n+1}, y_{n+2}, \dots, y_{n+m}\}$. When the
141 sentiment words belong to positive sentiment words. $y_i = 1$; and vice versa. $y_i = -1$. On the one
142 hand, the classification of sentiment words is reliant on the polarity information supplied by the
143 seed sentiment words. On the other hand, it is believed that sentiment words sharing the same
144 polarity are often associated with profound semantic similarity. Thus, the semantic similarity
145 interlinking the sentiment words to be classified can also serve as a valuable determinant of their
146 polarity.

147 Define the graph $G = \langle N, M \rangle, |N| = |S| + |W|$, where N is the set of G is the set of nodes in the
148 graph (nodes consist of all sentiment words). $|S|$ is the number of seed sentiment words. $|W|$ is
149 the number of sentiment words to be classified. $|W| \times |N|$ Linkage matrix M describes the linkage
150 relationship between nodes in the disjoint graph. M_{ij} is the number of nodes i and j semantic
151 similarity between nodes. M can be decomposed into $|W| \times |S|$ the submatrix of U and $|W| \times |W|$
152 the submatrix of V . U_{ij} represents the sentiment words to be measured i and the seed sentiment
153 word j semantic similarity between the sentiment word and the seed sentiment word. After
154 introducing the PageRank model, the iterative formula of the sentiment word polarity discriminant
155 algorithm is as follows:

$$Y_W^{(n)} = (1 - \beta)UY_S + \beta VY_W^{(n-1)} \quad (1)$$

156 Where $Y_W^{(n)}$ represents Y_W after n-th iterations. β is the weighting factor. $0 < \beta < 1$.

157

158 3.1.2 Improvement based on time factor

159 To mitigate the issue of lower PR value caused by fewer pages being linked to new content,
 160 this paper proposes the inclusion of a time feedback factor in the PageRank calculation formula.
 161 The time feedback factor compensates for the PR value of older pages, thereby improving the
 162 final recommendation order. The proposed method is based on the fundamental concept that a
 163 web page searched multiple times within the same search cycle should be counted only once.
 164 The inclusion of the time feedback factor in the PageRank calculation formula is expressed as
 165 follows:

$$W_t = e/T \quad (2)$$

166 Where. e/T is the expression for calculating the time feedback factor of a web page, which
 167 indicates the frequency of content searched by search engines. e is usually taken as $0.15/n$, n is
 168 the total number of web pages, and the size of e does not affect the distribution of the final PR
 169 value, but affects the iterative process of the algorithm, which can effectively improve the situation
 170 of low PR value of new pages.

171 The fundamental concept behind the proposed enhancement, which leverages both similarity
 172 and time factors, is to assign PR value based on the degree of similarity between the current web
 173 page and the linked pages, rather than a uniform assignment strategy. Additionally, a time
 174 feedback factor is incorporated to account for new web pages. The modified PageRank
 175 calculation formula is expressed as follows:

$$PR(u) = (1 - d) + d \cdot \left(\sum_v PR(v) + \alpha \cdot \text{Score}(q, D) \right) + W_t \quad (3)$$

176

177 3.2 Image emotion feature extraction based on improved ResNet

178 In this paper, we apply ECA to the residual network structure with the design idea of SE-
 179 ResNet network, and improve the optimization of ResNeXt50. The ECA mechanism is shown in
 180 Figure 2.

181

182 Figure 2. Schematic diagram of ECA attention mechanism

183 Assuming that any of the feature transformations including convolution is denoted as F_{tr} .
 184 $X \rightarrow U$, where $X \in R^{H \times W \times c}$, $U \in R^{H \times l \times c}$, then compress all global information in a channel descriptor
 185 using global averaging pooling (GAP), the spatial dimensionality $H \times W$ in shrinking feature U is
 186 used to generate statistical variables.

$$Z_n = F_{sq}(u_n) = \frac{1}{H \times W} \sum_i \sum_j u_n(i, j) \quad (4)$$

187 Where Z_n can be interpreted as a collection of local features whose statistical information can
 188 express the whole image and have a global field of perception. Statistics. The statistic Z does not
 189 require dimensionality reduction, and the attention of each channel can be obtained by the

190 following way. The weight size is used as the measure of attention.

$$\rho = \sigma(W_k \cdot Z) \quad (5)$$

191 Where W_k contains $k \times C$ parameters, which are defined as .

$$\begin{bmatrix} w_1^1 & \dots & w_1^k & 0 & 0 & \dots & \dots & 0 \\ 0 & w_2^2 & \dots & w_2^{k+1} & 0 & \dots & \dots & 0 \\ \vdots & \vdots & \vdots & \vdots & \ddots & \vdots & \vdots & \vdots \\ 0 & \dots & 0 & 0 & \dots & w_c^{c-k+1} & \dots & w_c \end{bmatrix} \quad (6)$$

192 where σ represents the sigmoid nonlinear activation function.

193 In this paper, 8 ResNeXt50 modules are stacked in series, and the ECA attention mechanism
194 is embedded after each ResNeXt50 module to capture the interdependent associations between
195 channels. It further enhances the image emotion feature extraction capability. The attention
196 weights of each channel after the ECA module are.

$$\rho = \sigma(H^{(k)} * F_{sq}(Q)) \quad (7)$$

197 In order to effectively avoid the degradation problem of deep networks, the idea of residuals
198 is introduced to weight each channel and add it to the original input features.

$$Y = (w \otimes Q) \oplus X \quad (8)$$

199 Where Y denotes the output feature map after a block. \otimes represents the corresponding dot
200 product of the elements. \oplus represents the corresponding sum of elements.

201 By integrating the ECA mechanism in DCNN, the network can be tailored to meet the specific
202 requirements of different depths. In shallow networks, this module enhances the quality of
203 extracted features at lower layers by highlighting informative features. In contrast, in deeper
204 networks, the significance of this module becomes more pronounced as the extracted features
205 become more strongly correlated with the target category.

206

207 3.3 Emotion feature integration

208 For the integration of emotion features between text and images. First, $f_\theta(X^i)$ is defined as
209 the input features X^i in the parameter θ and then estimate the probability distribution by the
210 Sigmoid function with Equation (9).

$$f_\theta(X^i) = \frac{1}{1 + e^{\theta^T X^i}} \quad (9)$$

211 Equation (9) defines the degree of bimodal contribution to the overall sentiment. ρ^T and ρ^T
212 are the weights of the text and picture contributions to the overall sentiment, respectively,
213 calculated as.

$$\begin{aligned}\rho^T &= f_\theta(X^T) - \frac{1}{2} \\ \rho^I &= f_\theta(X^I) - \frac{1}{2}\end{aligned}\quad (10)$$

214 Then the sentiment weight coefficients of the two modalities are compared to determine the
215 appropriate fusion strategy, which is calculated as follows.

$$X^c = \begin{cases} X^T \cup X^I & \text{if } \rho^T * \rho^I > 0 \\ X^T & \text{if } |\rho^T| - |\rho^I| \geq 0 \\ X^I & \text{if } |\rho^T| - |\rho^I| \leq 0 \end{cases}\quad (11)$$

216 Where X^c denotes the fused features. Sentiment classification is performed by fusing the
217 features of the text and image modalities, provided that the product of their respective sentiment
218 weights and sentiment weight coefficients is positive. If the absolute difference between the
219 sentiment weight coefficient values is greater than zero, the polarity of the sentiment is determined
220 based on the sentiment weight coefficient of the text modality.

221 The cross-modal learning algorithm calculates the predicted probability distribution of image
222 and text sentiment by Kullback-Leibler divergence. The sentiment probabilities of text and image
223 are discrete events, which are assumed to be defined as Event A and Event B, respectively.

$$D_{KL}(A \parallel B) = \sum_i P_A(x_i) \log \left(\frac{P_A(x_i)}{P_B(x_i)} \right)\quad (12)$$

224 The loss function of Sigmoid can be used to consider the loss between the expected estimate
225 and the true label, as well as related to the loss between the fusion characteristics of the graphical
226 features and the estimated distribution, as shown in Equation (13).

$$\begin{aligned}J(\theta) &= \frac{1}{N} \sum_{i=1}^N D\{Y_i \parallel f_{\theta^c}(X_i^c)\} + \frac{\alpha}{2} \theta^T \theta \\ &+ \frac{\beta}{N} \sum_{i=1}^N [D\{f_{\theta^c}(X_i^c) \parallel f_{\theta^T}(X_i^T)\} + D\{f_{\theta^c}(X_i^c) \parallel f_{\theta^I}(X_i^I)\}]\end{aligned}\quad (13)$$

227 Where $\theta = \{\theta^c, \theta^T, \theta^I\}$ represents the cross-modal learning parameters. α and β are the
228 superparameters of the model. $\frac{\alpha}{2} \theta^T \theta$ is the canonical term, to prevent overfitting of the model.

229

230 4 Experiment and analysis

231 4.1 Experimental setup

232 For the experimental corpus, a total of 814 positive sentiment words and 1,232 negative
233 sentiment words were selected from the HowNet Sentiment Dictionary. Prior to analysis, the data
234 were preprocessed by separating the words using JIBEAs for high-frequency word statistics and
235 mutual information model construction. Additionally, a user code mapping table was constructed
236 to ensure uniform coding across all users.

237 To facilitate the sentiment classification task, this paper employs the hyperparameter method
238 in ResNeXt network. The optimal kernel scale size for convolution is set at 3×3 , while the
239 quantization step is fixed at one. The optimal pooling size for the pooling layer is 2×2 , and the
240 quantization step is two. The hyperparameters were determined via tuning of the pre-trained
241 network using ResNeXt. The input images were normalized and have a maximum width of
242 256×256 pixels. Histogram equalization was used to achieve data enhancement.

243 To evaluate the effectiveness of the proposed algorithm, a comparative test was conducted
244 against several commonly used neural network models. These include:

245 (1) DCNN: This model utilizes one CNN to extract sentiment features from both the text and
246 image modalities separately, and predicts the sentiment polarity of each modality. The outputs
247 are then fused using an averaging strategy at the decision level.

248 (2) CCR: This model uses CNN to extract features from both the image and caption text, and
249 then employs KL scatter to learn the consistent sentiment of both modalities. This model is a
250 feature layer fusion approach.

251 (3) AttnFusion: This model uses BiLSTM to model video frame sequences and text
252 sequences, and an attention mechanism is used to learn the alignment weights between video
253 frames and text words. The features from both modalities are fused using this attention
254 mechanism to produce a more accurate multi-channel feature representation. The aligned multi-
255 peaked features are then fed into the sequence model for sentiment recognition.

256 (4) MDREA: This model employs two separate RNNs to encode data from image and text
257 inputs independently. An attention vector is generated by computing the weight parameter
258 between the image encoding vector and the text hidden state. The Softmax function is then
259 applied to the vector to predict the sentiment category.

260

261 4.2 Results and Discussion

262 The model utilizes cross-entropy as the loss function and employs the Adam optimizer as the
263 chosen optimization algorithm throughout the entirety of the training process. Figure 3 presents
264 the training outcomes.

265

266

Figure 3. Model training results

267 The examination reveals that there is negligible disparity between the accuracy of the test
268 set and that of the training set. Similarly, the loss value of the test set aligns with the loss value of
269 the training set, implying that the model is viable for practical applications.

270

271 4.2.1 Model comparison

272 The performance evaluation of the sentiment analysis model described in Section 4.1 is
273 presented in Figure 4 and Figure 5, in comparison with the art appreciation sentiment analysis
274 model introduced in this paper. The experimental assessment was conducted on two datasets
275 obtained from the Flickr and Twitter websites, and the evaluation metrics employed were
276 Precision, Recall, and F1.

277

278

Figure 4. Comparison of model performance on the Flickr dataset

279

280

Figure 5. Comparison of model performance on Twitter dataset

281

282

283

284

285

286

287

288

289

290

291

292 4.2.2 Emotion classification results

293

294

295

296

297

298

299

300

301

Figure 6. Emotion classification results on Flickr dataset

302

303

Figure 7. Emotion classification results on Twitter dataset

304

305

306

307

308

309

310

311

312

313

314

315

The proposed model surpasses the other four models in terms of Precision, Recall, and F1, as is evident from the figure. In fact, the Flickr dataset's accuracy improved by a substantial margin of 23.14%, 16.35%, 8.11%, and 4.26%, respectively, when compared to the other four methods. Moreover, the proposed model exhibits superior robustness, even when confronted with smaller Twitter datasets. It outperforms the other four models, thereby establishing the better classification results of the proposed model in the field of cross-modal graphical and textual fusion sentiment analysis. By fusing text features and image features, the model successfully leverages the correlation between different modalities, discovers deeper associations, and performs complementary sentiment information. This feature fusion approach also reduces discrepancies, further proving its feasibility and effectiveness on cross-modal data.

Figures 6 and Figure 7 present the confusion matrix results of the bimodal sentiment model. In the Flickr dataset, the model achieves an impressive probability of correct prediction for the four labels, namely "sad," "happy," "angry," and "neutral," with accuracy rates of 73.44%, 70.83%, 88.02%, and 59.38%, respectively. In comparison, the Twitter dataset has a higher prediction accuracy, albeit with a reduced recognition of the "happy" sentiment label. On the whole, the model demonstrates the highest recognition rate for angry labels, while its performance is weakest for neutral labels, which are frequently misidentified as sad labels.

The experimental results presented above provide evidence that the model proposed in this chapter performs exceptionally well across all evaluation indices. The proposed model not only achieves a high level of prediction accuracy for each sentiment label but also outperforms both unimodal and other bimodal sentiment analysis models in terms of classification performance and stability. Moreover, the proposed model exhibits remarkable generalization ability, further validating its effectiveness in the field of sentiment analysis.

311 4.3 Discussion

To summarize, the proposed model in this paper effectively improves the sentiment classification accuracy and achieves the best sentiment recognition ability. Additionally, the model's robustness and generalization ability have been significantly enhanced. Moreover, the addition of temporal feedback factors slightly improves the accuracy of the PageRank algorithm.

316 This is due to the fact that the temporal factor compensates for the PR value and ensures that
317 new high-quality content is appropriately ranked. The ECA-based attention mechanism has also
318 been successful in improving classification accuracy while reducing the number of model
319 parameters by enabling local cross-channel interaction of sentiment features through one-
320 dimensional convolution. Furthermore, the accuracy of the model in distinguishing between
321 Positive and Negative words differs significantly, which is largely due to the quality of seed word
322 selection. Although the number of seed words with different sentiments can be guaranteed to be
323 equivalent, the quality of the seeds cannot be guaranteed. Nonetheless, the experimental results
324 fully validate the feasibility of the proposed method. It is essential to emphasize that although the
325 connection weights for graph nodes in the algorithm description are calculated using HowNet,
326 other supervised or unsupervised methods can also be used to obtain the connection weights.

327 In specific application scenarios, teachers can guide students to analyze and appreciate
328 images, not only focusing on the surface content of the images, but also delving deeper into the
329 meaning behind them. Through online interactive comments, teachers can capture the different
330 emotions of individual learners towards the same artwork. With the increasing popularity of social
331 media, many users share their current developments on these platforms, which often reflect their
332 genuine emotions when posting messages. By analyzing such information, we can better
333 understand the interests and preferences of users at a particular period and predict future trends
334 based on user sentiment. This approach can also help in the development of art appreciation
335 software, which includes image loading (PhotoLoader), text loading (TextLoader), and prediction
336 results (ShowResult). The software's structure is shown in Figure 8.

337

338 Figure 8. Sequence diagram of art appreciation

339 The image loading function serves the purpose of loading the image content uploaded by the
340 user into a designated variable, carrying out the necessary pre-processing steps, and finally
341 utilizing the processed output as the input for the prediction result class. Similarly, the text loading
342 function is responsible for loading the user's input text content into a variable, executing the
343 required pre-processing and sentiment score vector transformation processes, and subsequently
344 utilizing the resultant output as an input for the prediction result class. The primary function of the
345 prediction result class is to combine the outputs from the image loading and text loading functions
346 and employ them as inputs to the sentiment analysis algorithm, thereby accomplishing sentiment
347 analysis of the fused graphical data.

348 5 Conclusion

349 This study proposes a method for determining the sentiment polarity of words based on the
350 PageRank model, which is employed as an input for text sentiment features in the fusion model.
351 Furthermore, inspired by the ResNeXt model, the main module of the deep sentiment feature
352 extraction network is designed as ResNeXt50, and each residual module is equipped with a BN
353 layer to expedite network convergence. The model's training outcomes on both the Flickr and
354 Twitter datasets indicate that the proposed model considerably improves sentiment classification
355 accuracy and achieves superior sentiment recognition capabilities, thereby enhancing the model's

356 robustness and generalization capacity. In practical applications, the decision layer fusion is
357 achieved by dynamic weight assignment, thereby completing the graphical fusion-based
358 sentiment analysis and facilitating the development and design of the appreciation module in
359 software. However, the paper's training network necessitates a substantial amount of labeled
360 sentiment data, which is currently unavailable on a large-scale and clearly labeled for graphical
361 sentiment analysis. By integrating and analyzing multimodal information such as text, image, and
362 speech-video, it is plausible that the unimodal problem can be resolved more effectively and
363 improve the efficiency of human-computer interaction.

364

365 **Acknowledgments**

366 I would like to thank my school for supporting my research.

367 **Conflicts of Interest**

368 The author has no conflict of interest.

369 **Funding Statement**

370 This work received no funding.

371 **Data Availability**

372 The dataset employed in this investigation is made readily available and accessible to interested
373 parties.

374

375 **References**

- 376 [1] Tan, C. T., & Ferguson, S. (2014). The role of emotions in art evaluation. *interactive experience*
377 *in the digital age: Evaluating new art practice*, 139-152.
- 378 [2] Yeh, S. L., Lin, Y. S., & Lee, C. C. (2019, May). An interaction-aware attention network for
379 speech emotion recognition in spoken dialogs. in *ICASSP 2019-2019 IEEE International*
380 *Conference on Acoustics, Speech and Signal Processing (ICASSP)* (pp. 6685-6689). IEEE.
- 381 [3] Rao, T., Li, X., & Xu, M. (2020). Learning multi-level deep representations for image emotion
382 classification. *neural processing letters*, 51, 2043-2061. Sharma
- 383 [4] Sharma, R., Pachori, R. B., & Sircar, P. (2020). Automated emotion recognition based on
384 higher order statistics and deep learning algorithm. *Biomedical Signal Processing and Control*,
385 58, 101867.
- 386 [5] Li, L., Zhu, H., Zhao, S., Ding, G., & Lin, W. (2020). Personality-assisted multi-task learning
387 for generic and personalized image aesthetics assessment. *IEEE Transactions on Image*

- 388 Processing, 29, 3898 -3910.
- 389 [6] Sharma, D., Dhiman, C., & Kumar, D. (2022, December). A Review of Stylized Image
390 Captioning Techniques, Evaluation Parameters, and Datasets. in 2022 4th International
391 Conference on Artificial Intelligence and Speech Technology (AIST) (pp. 1-5). IEEE.
- 392 [7] Mo, Y., Wu, Y., Yang, X., Liu, F., & Liao, Y. (2022). Review the state-of-the-art technologies
393 of semantic segmentation based on deep learning. *Neurocomputing*, 493, 626-646.
- 394 [8] Jiang, Y. G., Xu, B., & Xue, X. (2014, June). Predicting emotions in user-generated videos. in
395 Proceedings of the AAAI Conference on Artificial Intelligence (Vol. 28, No. 1).
- 396 [9] Niu, T., Zhu, S., Pang, L., & El Saddik, A. (2016). Sentiment analysis on multi-view social data.
397 in *MultiMedia Modeling: 22nd International Conference, MMM 2016, Miami, FL, USA, January 4-*
398 *6, 2016. Proceedings, Part II 22* (pp. 15-27). Springer International Publishing.
- 399 [10] Zhang, W., He, X., & Lu, W. (2019). Exploring discriminative representations for image
400 emotion recognition with CNNs. *IEEE Transactions on Multimedia*, 22(2), 515-523.
- 401 [11] Kumar, A., & Garg, G. (2019). Sentiment analysis of multimodal twitter data. *Multimedia Tools*
402 *and Applications*, 78, 24103-24119.
- 403 [12] Farkhod, A., Abdusalomov, A. B., Mukhiddinov, M., & Cho, Y. I. (2022). Development of Real-
404 Time Landmark-Based Emotion Recognition CNN for Masked Faces. *sensors*, 22(22), 8704.
- 405 [13] Li, H. (2021). Internet tourism resource retrieval using PageRank search ranking algorithm.
406 *Complexity*, 2021, 1-11.
- 407 [14] Talipu, A., Generosi, A., Mengoni, M., & Giraldi, L. (2019, June). Evaluation of deep
408 convolutional neural network architectures for emotion recognition in the wild. in 2019 IEEE 23rd
409 International Symposium on Consumer Technologies (ISCT) (pp. 25-27). IEEE.
- 410 [15] Roul, R. K., & Sahoo, J. K. (2021). A novel approach for ranking web documents based on
411 query-optimized personalized pagerank. *International Journal of Data Science and Analytics*,
412 11(1), 37-55.
- 413 [16] Chakrabarti, S. (2007, May). Dynamic personalized pagerank in entity-relation graphs. in
414 Proceedings of the 16th international conference on World Wide Web (pp. 571-580).
- 415 [17] Li, J., Chen, D., Yu, N., Zhao, Z., & Lv, Z. (2021). Emotion recognition of Chinese paintings
416 at the thirteenth national exhibition of fines arts in China based on advanced affective computing.
417 *frontiers in Psychology*, 12, 741665.
- 418 [18] Scozzafava, F., Maru, M., Brignone, F., Torrisi, G., & Navigli, R. (2020, July). Personalized
419 PageRank with syntagmatic information for multilingual word sense disambiguation. in
420 Proceedings of the 58th annual meeting of the association for computational linguistics: system
421 demonstrations (pp. 37-46).
- 422 [19] Gao, Y., Yu, X., & Zhang, H. (2020). Uncovering overlapping community structure in static
423 and dynamic networks. *Knowledge-Based Systems*, 201, 106060.
- 424 [20] Mo, D., & Luo, S. (2021, October). Agenda: Robust personalized pageranks in evolving
425 graphs. in Proceedings of the 30th ACM International Conference on Information & Knowledge
426 Management (pp. 1315-1324).
- 427 [21] Lamurias, A., Ruas, P., & Couto, F. M. (2019). PPR-SSM: personalized PageRank and
428 semantic similarity measures for entity linking. *bmc bioinformatics*, 20(1), 1-12.

- 429 [22] Liu, Q., Zhang, R., Liu, X., Liu, Y., Zhao, Z., & Hu, R. (2019). A novel clustering algorithm
430 based on PageRank and minimax similarity. *Neural Computing and Applications*, 31, 7769-7780.
- 431 [23] Zhu, T., Li, L., Yang, J., Zhao, S., Liu, H., & Qian, J. (2022). Multimodal sentiment analysis
432 with image-text interaction network. *IEEE Transactions on Multimedia*.
- 433 [24] Zhao, Z., Zhu, H., Xue, Z., Liu, Z., Tian, J., Chua, M. C. H., & Liu, M. (2019). An image-text
434 consistency driven multimodal sentiment analysis approach for social media. *Information
435 Processing & Management*, 56(6), 102097.
- 436 [25] Jiang, Y., Li, W., Hossain, M. S., Chen, M., Alelaiwi, A., & Al-Hammadi, M. (2020). A snapshot
437 research and implementation of multimodal information fusion for data-driven emotion
438 recognition. *information Fusion*, 53, 209-221.
- 439 [26] Li, L., Qin, S., Lu, Z., Zhang, D., Xu, K., & Hu, Z. (2021). Real-time one-shot learning gesture
440 recognition based on lightweight 3D Inception-ResNet with separable convolutions. *Pattern
441 Analysis and Applications*, 24(3), 1173-1192.

Figure 1

Art appreciation sentiment analysis model

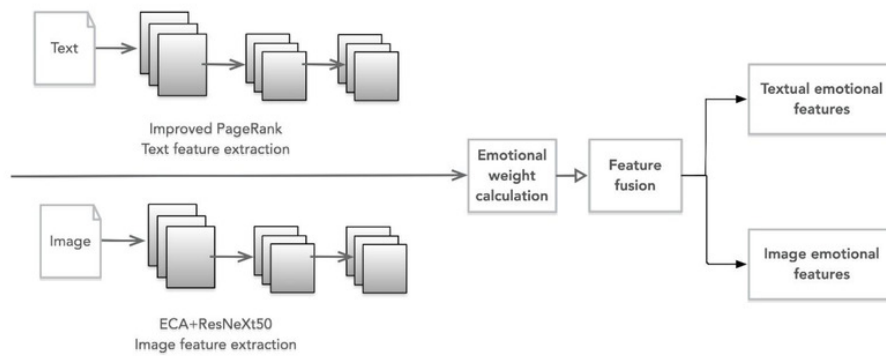


Figure 2

Schematic diagram of ECA attention mechanism

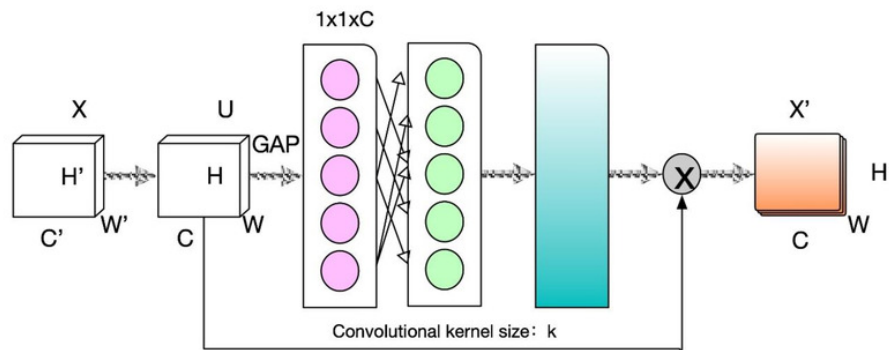


Figure 3

Model training results

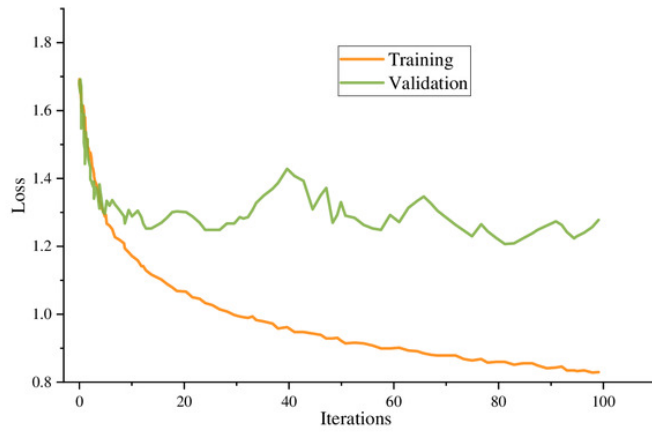


Figure 4

Comparison of model performance on the Flickr dataset

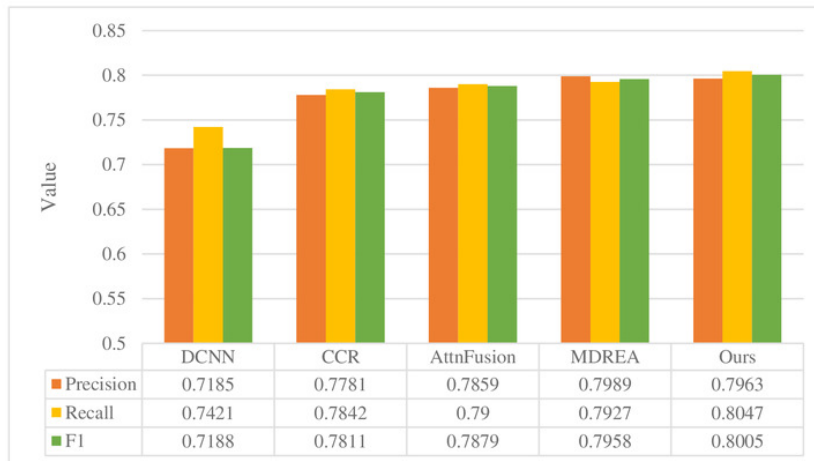


Figure 5

Comparison of model performance on Twitter dataset

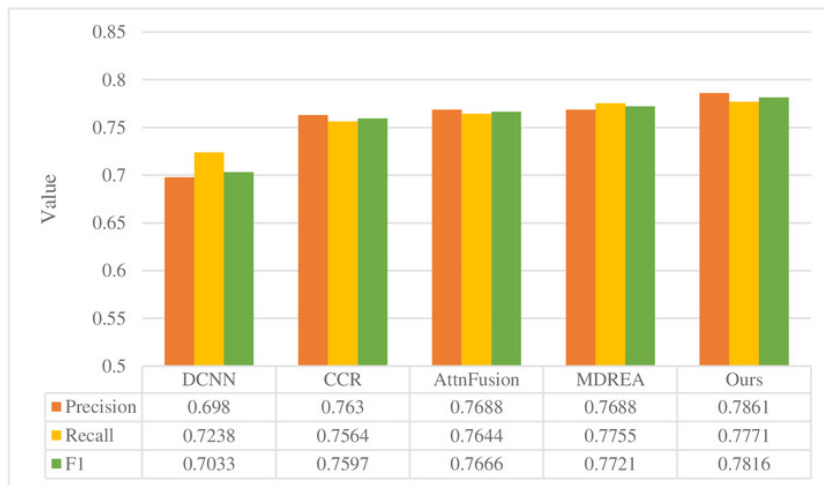


Figure 6

Emotion classification results on Flickr dataset

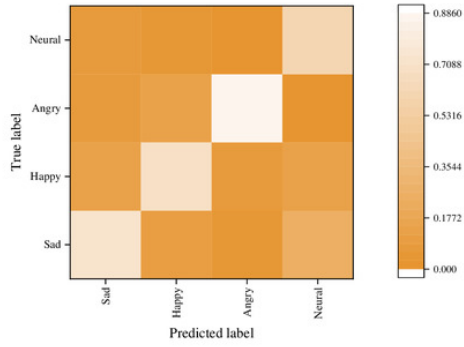


Figure 7

Emotion classification results on Twitter dataset

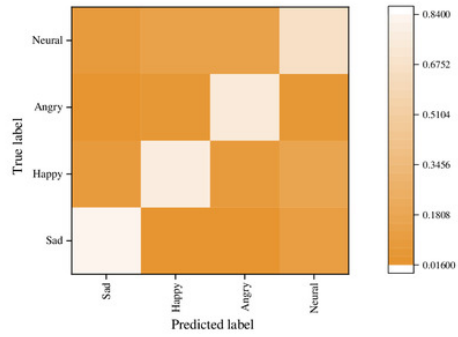


Figure 8

Sequence diagram of art appreciation

